Single Enzyme Direct Biomineralization of CdSe and CdSe-CdS Core-Shell Quantum Dots

Zhou Yang,[†] Li Lu,[‡] Christopher J. Kiely,[†,‡] Bryan W. Berger,[*,†,§] and Steven McIntosh[*,†]

[†]Department of Chemical and Biomolecular Engineering, Lehigh University, Bethlehem, Pennsylvania 18015, United States

[‡]Department of Materials Science and Engineering, Lehigh University, Bethlehem, Pennsylvania 18015, United States

[§]Program in Bioengineering, Lehigh University, Bethlehem, Pennsylvania 18015, United States

[*] Supporting Information

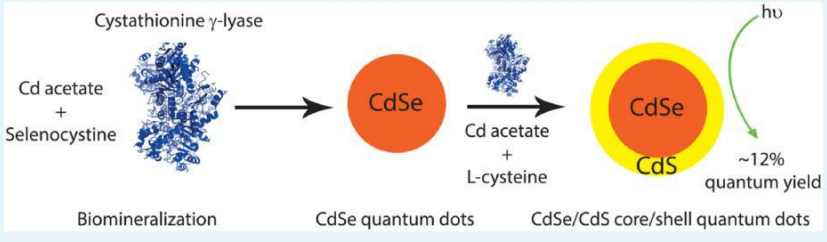

ABSTRACT: Biomineralization is the process by which biological systems synthesize inorganic materials. Herein, we demonstrate an engineered cystathionine γ-lyase enzyme, smCSE that is active for the direct aqueous phase biomineralization of CdSe and CdSe-CdS core-shell nanocrystals. The nanocrystals are formed in an otherwise unreactive buffered solution of Cd acetate and selenocystine through enzymatic turnover of the selenocystine to form a reactive precursor, likely H_2Se. The particle size of the CdSe core nanocrystals can be tuned by varying the incubation time to generated particle sizes between 2.74 ± 0.63 nm and 4.78 ± 1.16 nm formed after 20 min and 24 h of incubation, respectively. Subsequent purification and introduction of L-cysteine as a sulfur source facilitates the biomineralization of a CdS shell onto the CdSe cores. The quantum yield of the resulting CdSe-CdS core-shell particles is up to 12% in the aqueous phase; comparable to that reported for more traditional chemical synthesis routes for core-shell particles of similar size with similar shell coverage. This single-enzyme route to functional nanocrystals synthesis reveals the powerful potential of biomineralization processes.

KEYWORDS: single enzyme biomineralization, cadmium selenide, cadmium sulfide, quantum dot, core-shell, cystathionine γ-lyase

INTRODUCTION

Biomineralization, and related bioinspired synthesis routes, offers the potential for low temperature, aqueous phase synthesis of crystalline inorganic nanomaterials.[1,2] This stands in stark contrast to most traditional chemical approaches for nanoscale materials synthesis that require elevated temperatures and the use of environmentally unfriendly and costly solvents and reactants. Metal chalcogenide quantum dots (QDs) are perhaps the most frequently discussed biomineralized func-tional materials, with biomineralization reported to occur in a range of organisms.[3]

While these studies demonstrate feasibility, the primary outstanding challenge is to expand the accessible materials palette and tune size, composition, crystalline structure, and heterostructure combinations to reach the functional property metrics of comparative chemically synthesized materials. To this end, we are pursuing an approach termed single enzyme direct biomineralization where a single engineered enzyme is responsible for catalyzing mineralization and templating the quantum dot structure. In the current work, we report the first single enzyme direct biomineralization of CdSe and CdSe-CdS core-shell quantum dots with quantum yields that are equivalent to structurally similar chemically synthesized materials.

Nanocrystal synthesis requires addition or generation of reactive precursors and a templating/control mechanism to direct nanocrystal formation rather than larger, bulk particles. The most widely demonstrated bioinspired approaches seek to utilize biomolecules to template nanoparticle formation in aqueous solution upon addition of a chemical reactive precursor or solvothermal treatment.[3−9] For selenides and sulfides this is typically NaHSe, Na_2SeO_3, or Na_2S added to a solution of the metal salt and selected biomolecule. For example, Zhang et al. utilized a bovine serum albumin (BSA) to template the mineralization of Ag_2S paramagnetic quantum dots for tumor imaging.[10] Yang et al. extended this to demonstrate that BSA can also template CeO_2 nanoparticle mineralization.[11] This approach offers the advantage of fine control over templating, production of high-quality materials, and relatively simplified purification, but it requires the addition

of a chemically reactive precursor rather than utilizing a fully biological process.

An alternative approach is to utilize full organisms, or a large part of the cellular machinery, to biologically generate a reactive precursor and control growth. For example, bacteria-based biomineralization of size controlled CdS and PbS quantum dots has recently been demonstrated.[12−15] With regard to CdSe nanocrystals, biomineralization has been reported in bacterial, fungal, and yeast-based systems.[16−19] These approaches typically utilize the organism to reduce Se^{4+} in the water-soluble Na_2SeO_3 or $SeCl_4$ precursors to reactive Se^{2+} prior to reaction with a Cd salt. As an example, Cui et al. demonstrated intracellular CdSe nanocrystal synthesis within yeast cells, indicating that the reduction of Na_2SeO_3 forms organoselenium compounds, identified as selenocystine and selenomethio-nine.[16] In this case, size control of the quantum dots is suggested to be achieved by the controlled rate of reactive organoselenium generation leading to controlled intracellular growth of the quantum dots. While demonstrating a fully biological approach, intracellular synthesis mechanisms require subsequent cell lysis and harvesting of the nanocrystals from a complex mixture of biomolecules generated by the organism during synthesis. Fellowes et al. demonstrated ex-situ formation of CdSe with a bacterial route,[17] but, as with these other prior reports, no size control is demonstrated nor are quantum yields reported.

Our approach is to overcome the potential limitations of both prior strategies by utilizing single enzymes for both biological generation of reactive materials and nanocrystal templating in a strategy we term direct biomineralization.[20] This enables direct engineering of the enzyme toward control of the key mineralization and templating processes occurring within these complex systems while achieving biomineralization with the fewest possible components, in the current case, a Cd salt, an Se-containing precursor, and the enzyme in a buffered solution. In this specific case we also add 3-mercaptopropionic acid to stabilize the CdSe nanocrystals against photo-degradation in aqueous solution.[21] This approach decreases the number and complexity of subsequent purification steps required to obtain the quantum dot material, as cell lysis is avoided and only one biomolecule is present in solution. This intrinsically greener preparation route has the potential to simplify the synthesis process and reduce production cost.

Our previous studies reported an engineered strain of the bacteria Stenotrophomonas maltophilia (SMCD1) active toward the biomineralization of CdS, PbS, and PbS-CdS core-shell quantum confined nanocrystals.[12,13,15,20] Through identification and engineering of a cystathionine γ-lyase (smCSE) enzyme found associated with these nanocrystals, this procedure was simplified to a single enzyme approach for CdS biomineraliza-tion wherein we demonstrated that a single recombinant enzyme acts to both generate reactive sulfur via reduction of L-cysteine and template the formation of size controlled crystalline quantum dots.[20] This class of enzymes catalyze the formation of pyruvate, ammonia, and hydrogen sulfide from L-cysteine, providing the reactive sulfur precursor necessary for biomineralization.

In the current work, we demonstrate the first single enzyme approach to CdSe biomineralization from cadmium acetate and selenocystine. This simplified approach also lends itself to the synthesis of CdSe-CdS core-shell nanoparticles through subsequent biomineralization of a CdS shell onto the CdSe core. The resulting core-shell nanoparticles demonstrate the expected enhanced quantum yield compared to the core-only variant. The CdSe-based nanocrystals produced are also amenable to facile transfer to an organic phase for integration into quantum dot sensitized solar cells.

EXPERIMENTAL SECTION

Expression and purification of the recombinant smCSE enzyme was achieved according to the protocol reported in our previous paper.[11] In a typical procedure for CdSe synthesis, 1 mM cadmium acetate (99.999%, Alfa Aesar), 8 mM seleno-L-cystine (95%, Sigma-Aldrich), 20 mM 3-mercaptopropionic acid (MPA, 99%, Sigma-Aldrich), and 0.05 mg/mL smCSE enzyme in 0.05 M Tris-HCl buffer (pH = 9.0) were prepared in an N_2 atmosphere and sealed properly in a glovebox. The MPA was added as a stabilizing agent.[21] The mixture was then placed in the incubator for a specified time period between 20 min and 24 h with shaking at 37 °C. After synthesis, the CdSe nanocrystal solution was purified by centrifugation at 8000 rpm, followed by syringe filtration (0.2 μm) of the supernatant. The aqueous phase QD solutions thus obtained are referred to as harvested solutions. These harvested solutions were dialyzed (Snakeskin 3500 MWCO; Thermo Pierce) against ultrapure water to remove residual salts and are referred to hereafter as purified core particles.

CdS shell growth on the CdSe core was achieved by addition of 1 mM cadmium acetate (99.999%, Alfa Aesar), 8 mM L-cysteine (98%, Alfa Aesar), and 0.05 mg/mL of fresh smCSE enzyme to a 0.05 M Tris-HCl buffered (pH = 9.0) aqueous solution of purified CdSe QDs under N_2. The mixture was sealed and incubated with shaking at 37 °C for 12 h. The resulting CdSe-CdS QD solution was purified by centrifugation at 8000 rpm, followed by syringe filtration (0.2 μm) of the supernatant. The solution was further dialyzed (Snakeskin 3500 MWCO; Thermo Pierce) against ultrapure water to remove residual salts.

The biosynthesized aqueous soluble CdSe or CdSe-CdS QDs could be phase-transferred into 1-octodecene (ODE, 90%, Alfa Aesar) in the presence of an oleylamine (98%, Sigma-Aldrich) capping agent. In a typical experiment, 15 mL of the purified aqueous CdSe or CdSe-CdS QD sample was mixed with 5 mL of oleylamine and 10 mL of ODE. The solution was degassed for 10 min and then stirred vigorously under Ar for 1 h at 60 °C. The organic phase was further kept under inert conditions at 60 °C for another 12 h. The QDs were then precipitated by addition of ethanol, washed with ethanol, and resuspended in chloroform or toluene where they could be stored until ready for further use.

Ultraviolet (UV) illumination studies were conducted on these materials by exposing the phase transferred CdSe QDs to an 8 W UV lamp with an excitation wavelength of 312 nm. UV−vis absorption spectra (UV-2600, Shimadzu) and photoluminescence emission spectra (QuantaMaster 400, Photon Technology International) from the various colloids were also collected. Coumarin 153 (Sigma-Aldrich) in ethanol was used as a standard for the determination of quantum yields.[22] Samples for high angle annular dark field-scanning transmission electron microscopy (HAADF-STEM) imaging and X-ray energy dispersive spectroscopy (XEDS) analysis were prepared by drop casting QD suspensions onto holey carbon-coated copper or nickel TEM grids. The samples were analyzed in a 200 kV aberration corrected JEOL ARM 200CF analytical electron microscope equipped with a Centurio XEDS system.

Particle size analysis is complicated due to the nonspherical shape of the particles. A particle size distribution was determined by measuring the diameter of a circle that just fits within the width of the nanoparticles, since we are primarily interested in correlating the minimum physical dimension to the degree of quantum confinement exhibited by these particles.

QD sensitized solar cells were fabricated using commercially available glass slides coated with F-doped tin oxide (FTO, ~7 Ω/sq, Sigma-Aldrich). These substrates were covered with a TiO_2 blocking layer by dipping them into a 40 mM $TiCl_4$ (>99.0%, Sigma-Aldrich) solution, followed by sintering in air at 500 °C for 3 h. A second mesoporous TiO_2 film (TiO_2 paste, 27.0 wt %, Sigma-Aldrich) was

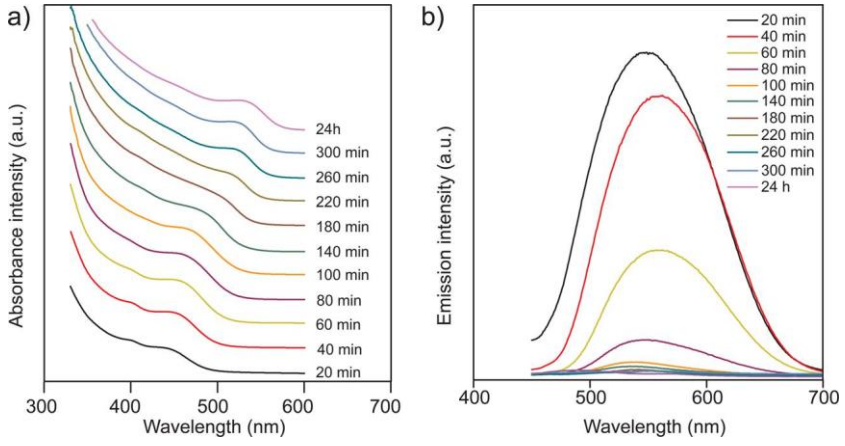

Figure 1. (a) UV−vis absorption and (b) corresponding fluorescence emission spectra of CdSe nanocrystals as a function of growth time in a buffered (pH = 9.0) aqueous solution of the smCSE enzyme, cadmium acetate, and selenocystine.

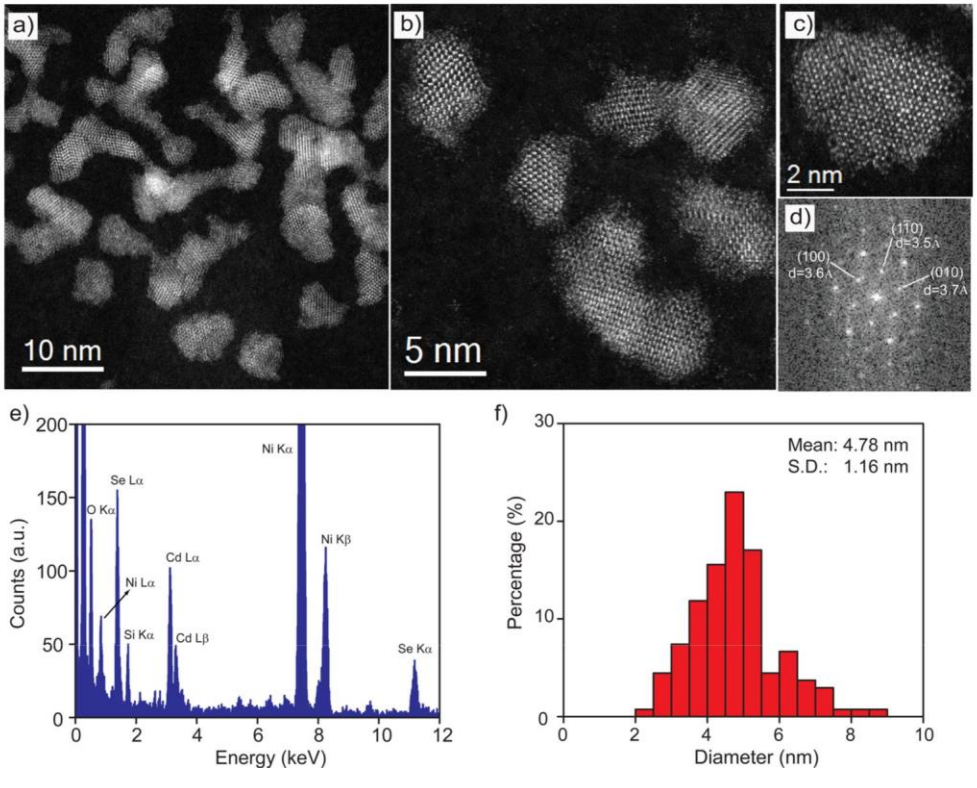

Figure 2. HAADF-STEM images (a−c), with corresponding FFT transform (d) of the particle in part c of biomineralized CdSe nanocrystals after 24 h growth. The XEDS spectrum (e) collected from an area of 130 nm × 160 nm confirms the presence of both Cd and Se. Particle size distribution (f) as determined from analysis of 138 particles.

deposited on top of the blocking layer with a doctor blade technique followed by sintering at 500 °C for 1 h in air. The CdSe QDs in chloroform were loaded into the mesoporous TiO_2 by drop-casting and allowing the solvent to evaporate. The completed photoelectrode was dried under ambient conditions. The counter electrode was prepared by painting a conductive gold paste (Electron Microscopy Sciences) onto FTO glass. The working and counter electrodes were assembled into a sandwich structure. The electrolyte was prepared by dissolving 0.5 M Na_2S (98%, Alfa Aesar), 0.5 M S (99.5%, Alfa Aesar), and 0.055 M NaOH (99.99%, Alfa Aesar) in water. The photocurrent density-versus-voltage (J−V) performance characteristic was measured using an electrochemical workstation (Reference 600, Gamry Instru-ments) under EM irradiation (AM 1.5 G solar simulator, model no. 10500, ABET Technologies) with an incident light intensity of 100 mW cm^{-2}.

RESULTS

Figure 1 shows the absorption and photoluminescence spectra of a buffered aqueous solution of smCSE enzyme, cadmium acetate, MPA, and selenocystine as a function of growth time. The absorption spectra show a clear first excitonic peak that red-shifts with increasing incubation time from 438 nm after 20 min to 535 nm after 260 min. Longer growth times lead to minimal further shift in the peak position. The peak absorption positions and red-shift with time are consistent with the expected trend for the nucleation and growth of CdSe quantum confined nanocrystals. The shift in the corresponding photo-luminescence spectra is smaller, with a peak position at 535 nm after 20 min of growth, shifting to 559 nm after 260 min. The

measured quantum yields, Figure S1, decrease from 0.8% for the sample with 20 min incubation time to 0.1% after 100 min incubation. Quantum yields determined for longer duration incubation times are below this 0.1% threshold. The relatively low quantum yields and large Stokes' shifts are both indicative of photoluminescence from deep surface traps and are very similar to that reported previously for CdSe prepared by synthesis utilizing Cd acetate and NaHSe as the reactive precursors.[5] This is likely due to both the formation of a relatively defective crystal structure with poor surface passivation. While the quantum yield values of these bare biomineralized CdSe nanocrystals in aqueous solution is low, they are still higher than some reported for purely chemical approach to CdSe nanocrystal synthesis in aqueous solution.[5]

The formation of CdSe nanocrystals is fully confirmed by HAADF-STEM imaging and X-ray energy dispersive spectros-copy (XEDS), as shown in Figure 2. The crystallites were phase transferred to 1-octodecene with oleylamine as a capping agent and further redispersed in chloroform to aid in sample preparation for STEM imaging. Figure 2a−c shows the HAADF-STEM images of the CdSe nanocrystals after 24 h growth. While the nanocrystals are rather irregular in shape, lattice fringes are visible. The lattice spacing and interplanar angles, as determined from the fast Fourier transform (FFT), Figure 2d, of the representative particle shown in Figure 2c, are consistent with the wurtzite structure of CdSe. The measured d-spacings of 0.35, 0.36, and 0.37 nm closely match the expected value of 0.37 nm for the $(1\bar{1}0)$, (100), and (010) planes of the wurtzite structured polymorph of CdSe when viewed along the [001] crystal projection. Similarly, the measured interplanar angles of 56.9°, 65.2°, and 57.9° are consistent within experimental error to the expected values of 60° for the wurtzite structure. Additional lattice fitting results are provided as Supporting Information, Figure S2 and Table S1. The associated XEDS analysis from an area containing approximately 200 particles confirms they are cadmium selenide, Figure 2e. The silicon and nickel signals also present in the spectrum are artifacts from the SDD-XEDS detector and Ni-mesh TEM grid, respectively.

The irregular shape of the nanocrystals makes direct interpretation of both the absorption and photoluminescence spectra somewhat problematical. The spherical equivalent diameter is 4.78 ± 1.16 nm, Figure 2f, for the sample grown for 24 h. The absorption peak position of 535 nm corresponds to a band gap energy of ~2.3 eV. The sizing curves for CdSe provided by Baskoutas and Terzis[23] and Yu et al.[24] indicate that the expected diameter for CdSe QDs with this band gap should be ~3 nm. This is relatively consistent with the ~4 nm shortest dimension of the irregularly shaped particles in Figure 2. It should be noted that these distributions are for as-synthesized materials without any size selection.

Nanocrystals isolated from the growth solution at shorter times show similar lattice fringe characteristics and the same characteristic irregular shapes as those particles incubated for longer time periods, Figure 3a. The mean size of 2.74 ± 0.63 nm, determined by fitting circles to the outline of 247 particles, Figure 3b, shows a reasonable correspondence to the expected size of ~2 nm for an absorption peak position of 438 nm.[23,24] Lattice fringes analysis, presented in Figure S3 and Table S2, demonstrates the presence of both zincblende and wurtzite polymorphs of CdSe in this instance.

It is important to note that these reported optical properties and nanocrystal formation are only evident upon incubation of

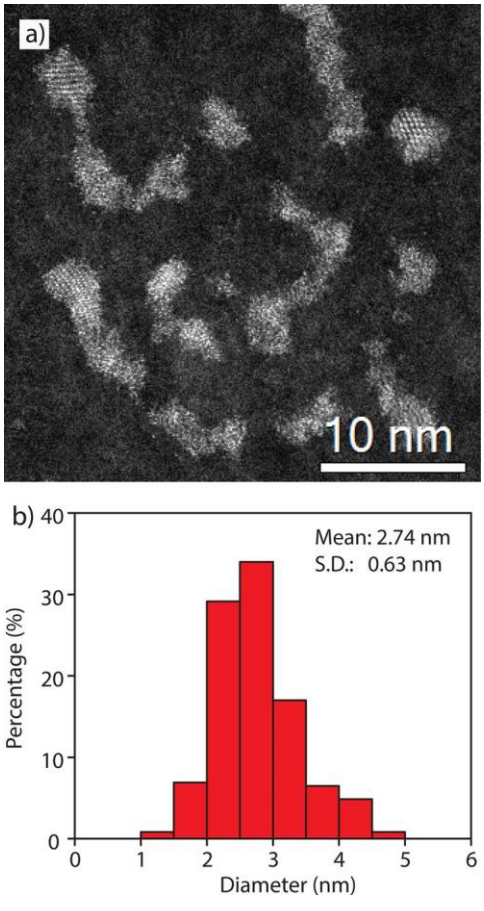

Figure 3. HAADF-STEM image (a) and corresponding particle size distribution (b) from 247 particles of biomineralized CdSe nanocryst-als after 20 min growth.

solutions containing all of the required components, namely, the smCSE enzyme, cadmium acetate, and selenocystine, Figure S4. The absence of enzyme or selenocystine yields no observed absorption, while the absence of cadmium acetate yields a broad absorption peak with a brown colored solution, consistent with the formation of selenium (Figure S4b,c).

As shown in Figure S1, the as-synthesized CdSe nanocrystals have a very low quantum yield, particularly as the mean particle size increases, most likely due to the presence of deep surface traps. One route to enhancing the quantum yield is to expose the phase transferred material to a UV source to deliberately photocorrode the particles. This UV "annealing" process is thought to increase quantum yield through surface restructur-ing during corrosion but also decreases the average particle size, as evidenced by a blue-shift in the absorption and photo-luminescence peak positions, Figure 4. The quantum yield is found to increase while the mean particle size decreases with increasing UV exposure time. The maximum quantum yield achieved through this approach was ~1.5% and extended exposure to the UV source appears to fully corrode the particles, leading to the almost complete disappearance of the UV−vis absorption peak.

A more promising approach to enhance the quantum yield of these biomineralized CdSe nanocrystals is through the growth of a surface passivating CdS shell.[25] Herein, consistent with the goal of producing functional materials by biomineralization, we have attempted enzyme mediated biomineralization of a CdS shell onto preformed core materials,[15] more specifically onto

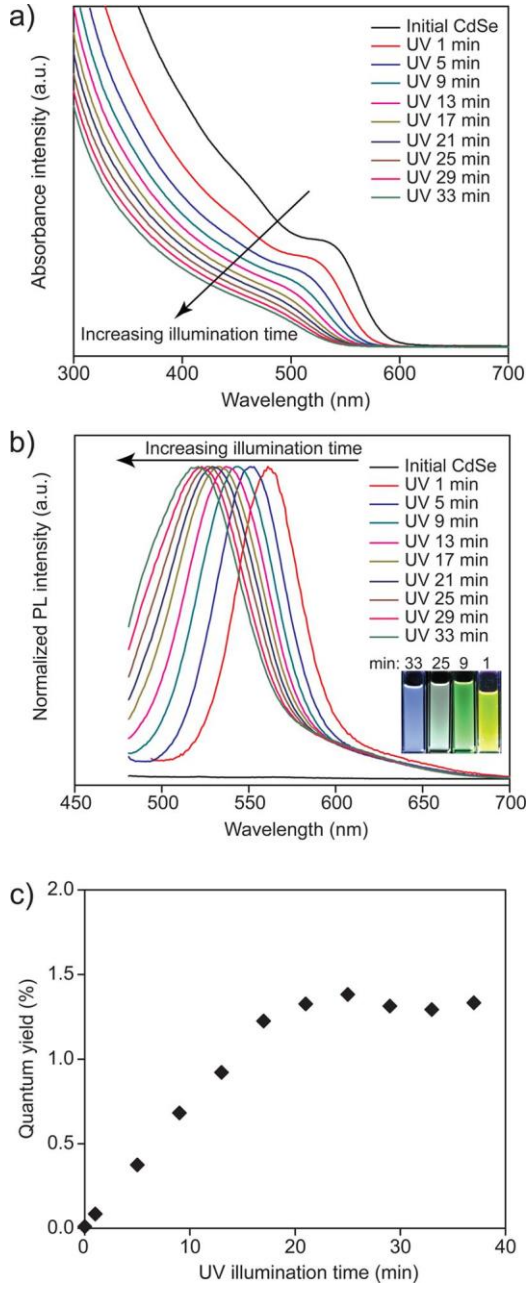

Figure 4. (a) UV−vis absorption spectra, (b) fluorescence spectra using a 420 nm excitation wavelength (inset photo exhibits the samples with 33, 25, 9, and 1 min from left to right under UV lamp), and (c) quantum yield of biomineralized CdSe nanocrystals as a function of time under UV illumination.

4.78 ± 1.16 nm and 2.74 ± 0.63 nm biomineralized CdSe nanocrystals. This second aqueous phase biomineralization step was initiated through the addition of fresh smCSE enzyme, Cd acetate, and L-cysteine to an aqueous solution of purified CdSe nanocrystals. The materials were incubated for 12 h to initiate shell growth. Figure 5 shows the absorption and photoluminescence spectra of CdSe core and CdSe-CdS core-shell nanocrystals formed on two sizes of CdSe core materials. The core materials correspond to those shown in Figures 1−3.

The quantum yield for both sets of materials increases substantially upon shell growth, as indicated by the significant increase in photoluminescence of the core-shell materials when compared to the corresponding core-only nanocrystals. This enhancement occurs in spite of a decrease in measured absorption intensity due to dilution of the nanocrystals upon addition of the enzyme, salt, and buffer solutions required to initiate shell growth. The quantum yield of the smaller 20 min growth time CdSe cores increases from 0.8% to 12%, while that of the larger 24 h growth time cores increases from almost 0 to 2.7% upon growth of the CdS shell. It should be noted there is a no significant red-shift in absorption and only a small blue-shift in photoluminescence peak position upon shell growth. For the 20 min growth core CdSe, the absorption and emission peaks are at 432 and 537 nm, respectively, shifting to 433 and 522 nm, respectively, after CdS shell growth. We note that these apparent shifts in peak position are very small when compared to the full width at half-maximum, ~125 nm, of the peaks and are indicative of a very thin or incomplete shell coverage. Full interpretation of the origin of this shift is complicated by the irregular shape of the nanocrystals, the presence of L-cysteine that can now act as a capping agent for the CdS shell,[12,13] and the existence of an incomplete shell.

Bright field (BF) and HAADF-STEM images of the larger core-shell particles following phase transfer to chloroform with oleylamine as capping agent, Figure 6, show nanocrystals with clear lattice fringes matching the wurtzite polymorph of CdSe, as expected from the analysis of the corresponding pure CdSe cores. Detailed lattice fringes analysis is provided in Figure S5 and Table S3. The particles maintain the irregular shape of the core materials. No clear core-shell boundary can be observed due to the relatively thin shell, the small difference in lattice parameters between CdSe and CdS, and the similarity in scattering power between S and Se. The mean particle size of these larger CdSe-CdS core-shell QDs shows an increase in mean particle size from 4.78 ± 1.16 nm to 5.29 ± 1.56 nm. This relatively small increase in mean diameter of 0.51 nm over the core material would suggest the formation of an approximately 0.7 monolayer thick shell if we ignore the potential for interdiffusion or displacement of Se by S. As noted by Peng et al.,[25] the 3.9% lattice mismatch between CdSe and CdS is likely small enough to allow epitaxial growth but large enough to limit interdiffusion.

XEDS spectra collected from individual nanocrystals confirms the coexistence of cadmium, selenium, and sulfur in all analyzed particles, Figure 5c and Figure S6.[26] Note that these particles have been phase transferred to the organic phase from the aqueous synthesis, with capping agent exchange from L-cysteine to oleylamine in order to remove any sulfur containing ligands that could have led to ambiguity in the source of the sulfur signal in our XEDS analysis. The calculated atomic ratios of Cd/Se/S from quantitative XEDS analysis for a single nanocrystal, Figure S6, is consistent with an equivalent shell thickness of 0.3 monolayers, in good agreement with the measured increase in mean particle size distribution.

Similar imaging and analysis of the smaller core-shell particles, where the shell is grown on CdSe nanocrystals incubated for only 20 min, show a similar result, Figure 7 and Figures S7 and S8. Figure S7 shows a nanocrystal with lattice fringes matching the zincblende polymorph of CdSe. The particle size distribution indicates an increase in mean size of 0.47 nm to 3.21 ± 0.90 nm after shell growth. This increase in diameter is consistent with that of the larger particles, reflecting the common growth period of 24 h utilized for shell growth. In this instance, this corresponds to 0.7 monolayers of pure CdS, although again we cannot rule out mixing of S and Se. Again, single nanocrystal XEDS analysis again confirms the coex-

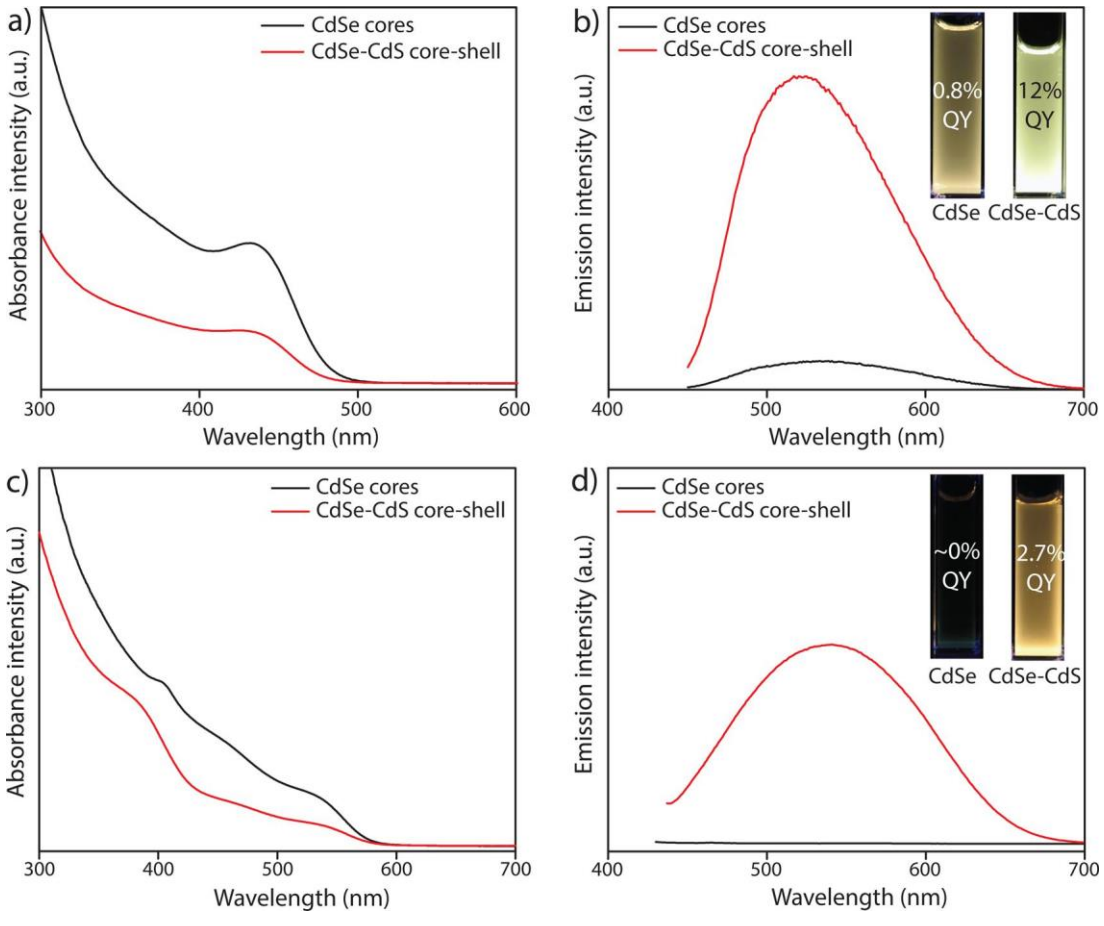

Figure 5. (a and c) UV−vis absorption and (b and d) fluorescence emission spectra of aqueous phase biomineralized CdSe core and CdSe-CdS core-shell nanocrystals. The insets show photographs of the solutions under UV illumination. Panels a and b show data for the 2.74 ± 0.63 nm CdSe cores, while panels c and d show similar data for the 4.78 ± 1.16 nm CdSe cores.

istence of Cd, S, and Se in each particle and quantitative XEDS analysis indicates the presence of 1.1 monolayer equivalent of CdS, in agreement with the value obtained from the increase in average particle size (Figure S8).

As a demonstration that these biomineralized CdSe quantum dots have potential in application, CdSe QDs grown for 20 min were phase transferred to chloroform and integrated into a TiO_2 electrode via drop casting to form a quantum dot sensitized solar cell. The performance characteristics of the resultant cell are shown in Figure 8. The addition of the biomineralized CdSe QDs leads to both increased open circuit voltage, V_{OC}, from 0.32 to 0.54 V, and increased short circuit current density, J_{SC}, from 0.41 to 0.88 mA/cm^2. This measured V_{OC} is consistent with previous reports for chemically synthesized CdSe quantum dot sensitized solar cells.[27,28] The corresponding fill factor increases from 41% to 48% upon CdSe QD incorporation. We have also provided a C−V performance curve for a similar cell sensitized with CdSe-CdS core-shell nanoparticles. As expected, the addition of the core-shell nanocrystals leads to minimal change from the blank state due to the confining effect of the CdS shell. It should be noted that these photovoltaic cells are not fully optimized and serve only to illustrate a route through which we may apply these biomineralized functional QD materials.

DISCUSSION

This work demonstrates the activity of cystathionine γ-lyase (smCSE) toward direct biomineralization of CdSe quantum confined nanocrystals in aqueous solution from cadmium acetate and selenocystine. We suggest that their formation mechanism is similar to that which we have previously demonstrated for CdS and PbS quantum dot biomineralization utilizing the same enzyme. In the case of these sulfides, the smCSE enzyme plays two critical roles. First, reactive sulfur species are generated from the decomposition of L-cysteine. The smCSE is a cystathionine γ-lyase, a class of enzyme active for the turnover of L-cysteine to form H_2S, NH_3, and pyruvate. Second, the enzyme plays a role in templating the growth of the nanocrystals.[20] We term this combination "single enzyme direct biomineralization" to reflect this dual role and the active turnover of otherwise inert solutions to form these functional nanocrystals.

We propose that CdSe biomineralization is induced by the enzymatic decomposition of selenocystine to form reactive H_2Se that then reacts with the Cd^{2+} ions in solution to form CdSe. This is analogous to the aqueous phase chemical synthesis routes that utilize NaHSe or H_2Se as the reactive selenium source. However, unlike L-cysteine which exists as a monomer under our synthesis conditions, the selenium analogue, selenocysteine, is added to solution as a dimeric species. The pK_a of the selenol group on selenocystine is 5.2 compared with 8.5 for the thiol group of L-cysteine.[29] Thus,

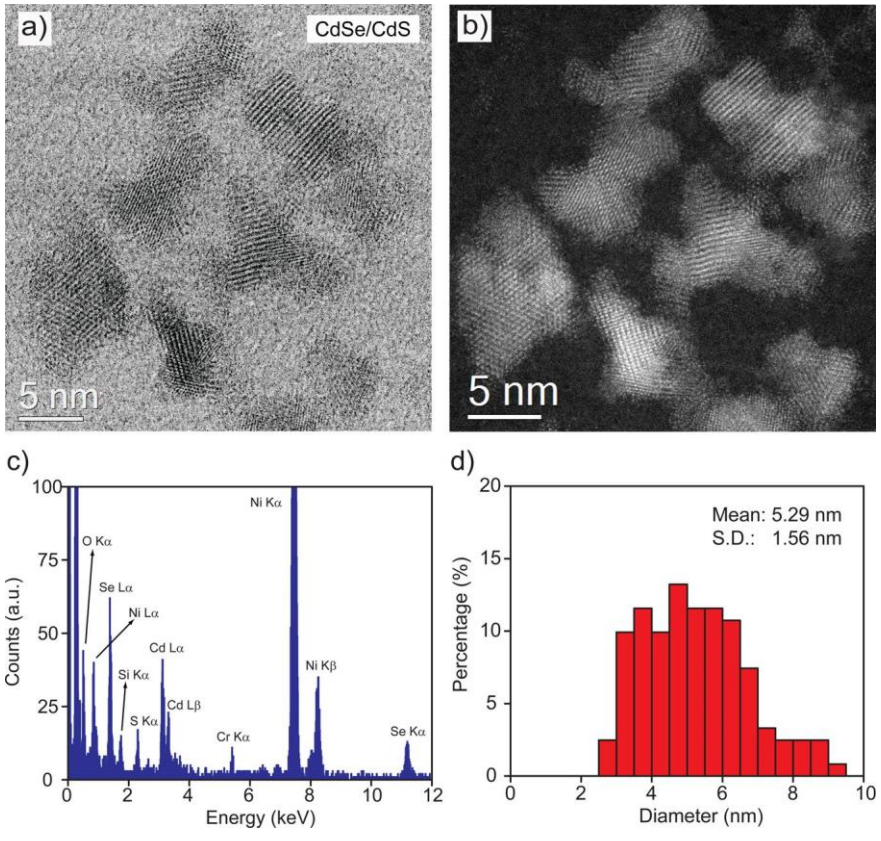

Figure 6. (a) Bright field (BF) and (b) HAADF-STEM images of the CdSe-CdS core-shell QDs grown utilizing the larger CdSe cores shown in Figure 2; (c) XEDS spectrum obtained from a single particle, confirming the coexistence of Cd, Se and S; and (d) particle size distribution was derived from measurements on 122 particles.

decomposition of selenocystine to form reactive H_2Se requires an initial dimer cleavage step when compared to the sulfur analogue.

Figure S4 demonstrates that a solution of only the smCSE enzyme and selenocystine forms selenium crystals, supporting the concept that smCSE is active toward the generation of reactive Se species from selenocystine. This hypothesis is further supported by the work of Esaki et al., who reported that cystathionine γ-lyase is active toward decomposition of the similar selenocystathionine dimer to form selenohomocysteine, selenocysteine, pyruvate α-ketobutyrate, and NH_3 and is active for the decomposition of these selenium containing products to H_2Se.[30]

Nanocrystal synthesis requires both this supply of a reactive precursor and a control of crystallite growth. The absence of the latter leads to the formation of bulk material rather than nanocrystals of defined size. Both L-cysteine and smCSE are active in controlling growth during CdS biomineralization as L-cysteine can act as a capping agent to stabilize CdS quantum dots in the aqueous phase. This combined control leads to the formation of relatively spherical nanocrystals. This stands in contrast to the more irregular shape observed for biomineral-ized CdSe in this study. This is most likely due to the relative absence of a capping agent during synthesis; as discussed above, the selenium precursor is in a dimeric form, selenocystine, which cannot act as a capping agent. Thus, only the smCSE enzyme is exerting control over crystallite growth, preventing the formation of bulk CdSe but leading to rather irregularly shaped nanocrystals. The very low quantum yield of the larger particles may be due to both the increased shape irregularity and potential aggregation of the nanocrystals due to relatively poor capping as the particle size increases. We deliberately avoided the addition of the commonly utilized L-cysteine or glutathione capping agents when preparing CdSe QDs as the presence of either would inevitably lead to the formation of CdS. Tuning of the templating action of smCSE is an area of ongoing work.

Unfortunately direct imaging to demonstrate a core-shell structure is not feasible and, as with other studies of similar materials, we must rely on indirect evidence for the structure. The substantial increase in quantum yield is perhaps the strongest evidence for the formation of a core-shell structure.[31,32] The 12% quantum yield reported here for the core-shell structure is substantially higher than that for the CdSe core nanocrystal and higher than we have achieved for CdS nanocrystals utilizing smCSE catalyzed biomineraliza-tion.[12,13] The single particle XEDS analysis in Figure 6c further confirms the coexistence of Cd, Se, and S within a single particle, indicating sequential mineralization of CdSe and CdS in a single particle rather than the formation of a secondary population of CdS particles. We would expect to observe a significant second absorption edge at ~375 nm if a significant separate CdS population were to be formed and, as stated, this secondary population would not yield such an increase in quantum yield. While small secondary peaks around this position are present in the absorption spectra for the smaller CdSe-CdS particles, these peaks are also present in the absorption spectra of the CdSe cores and are due to additional absorption peaks in the quantum confined core nanocrystals.[33] Finally, while the change in average diameter is within the

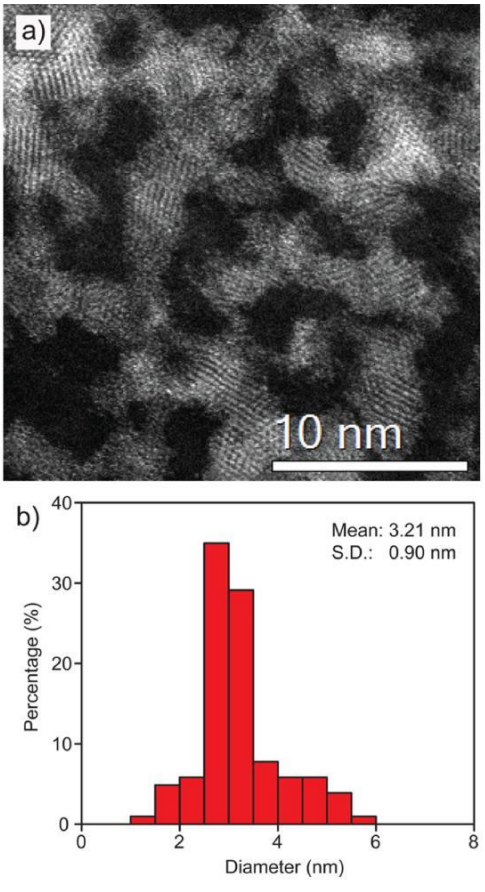

Figure 7. (a) HAADF-STEM image and (b) corresponding particle size distribution from 100 particles of biomineralized CdSe-CdS core-shell nanocrystals grown utilizing the CdSe core particles shown in Figure 3.

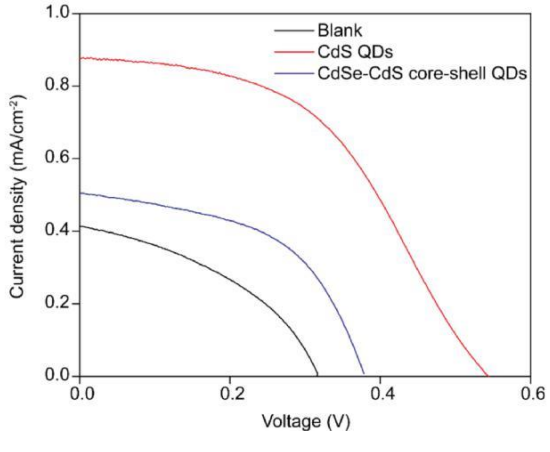

Figure 8. Current−voltage characteristics of the CdSe and CdSe-CdS core-shell quantum dot sensitized solar cells measured under one-sun illumination (AM 1.5 G, 100 mW/cm^2).

standard deviation, we have measured over 100 particles in each case and it should be noted that the diameter increases for both the smaller and larger CdSe cores upon shell growth and the magnitude of the increase is in-line with the shell thickness calculated from the XEDS data.

It is noteworthy that in the CdSe 24 h growth and CdSe-CdS core-shell 24 h core growth samples, the crystal structure of CdSe appears to be exclusively wurtzite, as suggested by lattice fringes analysis. We were unable to locate any particles that could unambiguously be fit to the zinc-blend structure in these samples. When the incubation time is reduced for both CdSe-only and CdSe-CdS core-shell samples, both wurtzite and zincblende CdSe polymorphs are identifiable in our analysis. This may originate from the difficulty for nanocrystal growth to reach thermodynamic equilibrium within a short time frame under such mild growth conditions. While there are suggestions that lower temperatures could favor formation of the zinc-blend structure,[34] the lower temperature in this study is 350 °C compared to 37 °C in the current work. It is also possible that the enzyme-induced crystallization and selenocystine binding characteristics could contribute to determining the preferred crystal structure. Control over the preferred structure is an ongoing focus of our research.

The formation of a CdS shell on the CdSe nanocrystals leads to substantial increase in quantum yield even with the estimated incomplete coverage of the shell over the core. While relatively thick CdS shells will lead to a significant red-shift in the absorbance and emission peak positions, incomplete or single monolayers are insufficient to significantly influence the band gap.[25,35] The quantum yields obtained are quite similar to those reported during the early years of organic phase chemical synthesis of metal chalcogenide quantum dots. For example, the quantum yields as a function of CdS coverage on CdSe cores reported by Peng et al.[25] They reported quantum yields in organic solution of 14% for 0.77 CdS monolayer coverage of 2.3 nm CdSe cores and 8% for 0.54 CdS monolayer coverage on 3.0 nm CdSe cores. This compares well with the 12% quantum yield we measured for the biomineralized 2.74 nm CdSe cores with 0.7 monolayers of CdS coverage. While substantial improvements in the size and shape uniformity and resulting optical properties of high temperature, organic phase, chemically synthesized materials have been achieved over the past 2 decades, with reported quantum yields exceeding 90%,[31] room temperature single enzyme aqueous phase quantum dot biomineralization is in its comparative infancy and will undoubtedly undergo further optimization as the technology matures.

We can also compare these materials to those produced chemically in the aqueous phase. Qian and Ren reported a 23% QY for CdSe-CdS alloy QDs formed through microwave assisted chemical synthesis in the aqueous phase.[36] Kalasas et al. reported greater than 40% QY for aqueous synthesized CdSe.[37] These comparisons demonstrate that, while in the relatively early stages of development and with some way to go, the biomineralized materials hold the promise to achieve functional equivalence with their chemically synthesized counterpart materials. Improvements in biomineralization based strategies are required if we are to fully overcome the challenges imposed by both the lower synthesis temperature and use of the aqueous phase to achieve greener synthesis of these materials while simultaneously achieving high performance metrics.

CONCLUSIONS

In summary, smCSE enzyme is capable of controlled CdSe nanocrystal synthesis directly from aqueous solution by using selenocystine and cadmium acetate as reactants. Furthermore, a CdS shell can be successfully grown onto CdSe seeds in the presence of smCSE enzyme to form a core-shell CdSe-CdS nanocrystals with significantly enhanced photoluminescence. This versatile enzyme demonstrates great potential for the synthesis of a variety of nanocrystal types and in principle can

be exploited for the large-scale production of QD nanocrystals with good functional properties.

ASSOCIATED CONTENT

* Supporting Information

Quantum yield of CdSe as a function of incubation time, additional HAADF-STEM images and lattice fitting, BF-STEM images and additional XEDS analysis, and UV− vis absorbance spectra of solutions in absence of key components (PDF)

AUTHOR INFORMATION

Corresponding Authors

*E-mail: mcintosh@lehigh.edu.

*E-mail: berger@lehigh.edu.

ORCID

Li Lu: 0000-0002-6688-1176

Steven McIntosh: 0000-0003-4664-2028

Notes

The authors declare no competing financial interest.

ACKNOWLEDGMENTS

This material is based upon work supported by the National Science Foundation under the EFRI-PSBR program, Grant No. 1332349. Additional support was received from the Lehigh University Collaborative Research Opportunity (CORE) program.

REFERENCES

(1) Mann, S.; Heywood, B.; Rajam, S.; Wade, V. Molecular Recognition in Biomineralization. In Mechanisms and Phylogeny of Mineralization in Biological Systems; Springer: New York, 1991; pp 47− 55.

(2) Nudelman, F.; Sommerdijk, N. A. Biomineralization as an Inspiration for Materials Chemistry. Angew. Chem., Int. Ed. 2012, 51, 6582−6596.

(3) Zhou, J.; Yang, Y.; Zhang, C. Toward Biocompatible Semiconductor Quantum Dots: From Biosynthesis and Bioconjugation to Biomedical Application. Chem. Rev. 2015, 115, 11669−11717.

(4) Spoerke, E. D.; Voigt, J. A. Influence of Engineered Peptides Cadmium Sulfide Nanocrystals. Adv. Funct. Mater. 2007, 17, 2031− 2037.

(5) Rogach, A. L.; Kornowski, A.; Gao, M.; Eychmuller, A.; Weller, H. Synthesis and Characterization of a Size Series of Extremely Small Thiol-Stabilized CdSe Nanocrystals. J. Phys. Chem. B 1999, 103, 3065−3069.

(6) Singh, S.; Bozhilov, K.; Mulchandani, A.; Myung, N.; Chen, W. Biologically Programmed Synthesis of Core-Shell CdSe/ZnS Nano-crystals. Chem. Commun. 2010, 46, 1473−1475.

(7) Liu, L.; Zhang, X.; Liu, X.; Liu, J.; Lu, G.; Kaplan, D. L.; Zhu, H.; Lu, Q. Biomineralization of Stable and Monodisperse Vaterite Microspheres Using Silk Nanoparticles. ACS Appl. Mater. Interfaces 2015, 7, 1735−1745.

(8) McMaster, W. A.; Wang, X.; Caruso, R. A. Collagen-Templated Bioactive Titanium Dioxide Porous Networks for Drug Delivery. ACS Appl. Mater. Interfaces 2012, 4, 4717−4725.

(9) Susapto, H. H.; Kudu, O. U.; Garifullin, R.; Yılmaz, E.; Guler, M. O. One-Dimensional Peptide Nanostructure Templated Growth of Iron Phosphate Nanostructures for Lithium-Ion Battery Cathodes. ACS Appl. Mater. Interfaces 2016, 8, 17421−17427.

(10) Zhang, J.; Hao, G.; Yao, C.; Yu, J.; Wang, J.; Yang, W.; Hu, C.; Zhang, B. Albumin-Mediated Biomineralization of Paramagnetic NIR Ag_2S QDs for Tiny Tumor Bimodal Targeted Imaging in vivo. ACS Appl. Mater. Interfaces 2016, 8, 16612−16621.

(11) Yang, Z.; Luo, S.; Zeng, Y.; Shi, C.; Li, R. Albumin-Mediated Biomineralization of Shape-Controllable and Biocompatible Ceria Nanomaterials. ACS Appl. Mater. Interfaces 2017, 9, 6839−6848.

(12) Yang, Z.; Lu, L.; Berard, V. F.; He, Q.; Kiely, C. J.; Berger, B. W.; McIntosh, S. Biomanufacturing of CdS Quantum Dots. Green Chem. 2015, 17, 3775−3782.

(13) Yang, Z.; Lu, L.; Kiely, C. J.; Berger, B. W.; McIntosh, S. Biomineralized CdS Quantum Dot Nanocrystals: Optimizing Synthesis Conditions and Improving Functional Properties by Surface Modification. Ind. Eng. Chem. Res. 2016, 55, 11235−11244.

(14) Marusak, K.; Feng, Y.; Eben, C.; Payne, S.; Cao, Y.; You, L.; Zauscher, S. Cadmium Sulphide Quantum Dots with Tunable Electronic Properties by Bacterial Precipitation. RSC Adv. 2016, 6, 76158−76166.

(15) Spangler, L. C.; Lu, L.; Kiely, C. J.; Berger, B. W.; McIntosh, S. Biomineralization of PbS and PbS−CdS Core−Shell Nanocrystals and their Application in Quantum Dot Sensitized Solar Cells. J. Mater. Chem. A 2016, 4, 6107−6115.

(16) Cui, R.; Liu, H.; Xie, H.; Zhang, Z.; Yang, Y.; Pang, D.; Xie, Z.; Chen, B.; Hu, B.; Shen, P. Living Yeast Cells as a Controllable Biosynthesizer for Fluorescent Quantum Dots. Adv. Funct. Mater. 2009, 19, 2359−2364.

(17) Fellowes, J. W.; Pattrick, R.; Lloyd, J.; Charnock, J. M.; Coker, V. S.; Mosselmans, J.; Weng, T.; Pearce, C. I. Ex-Situ Formation of Metal Selenide Quantum Dots using Bacterially Derived Selenide Precursors. Nanotechnology 2013, 24, 145603−145612.

(18) Kumar, S. A.; Ansary, A. A.; Ahmad, A.; Khan, M. Extracellular Biosynthesis of CdSe Quantum Dots by the Fungus, Fusarium Oxysporum. J. Biomed. Nanotechnol. 2007, 3, 190−194.

(19) Park, T. J.; Lee, S. Y.; Heo, N. S.; Seo, T. S. In Vivo Synthesis of Diverse Metal Nanoparticles by Recombinant Escherichia Coli. Angew. Chem., Int. Ed. 2010, 49, 7019−7024.

(20) Dunleavy, R.; Lu, L.; Kiely, C. J.; McIntosh, S.; Berger, B. W. Single-Enzyme Biomineralization of Cadmium Sulfide Nanocrystals with Controlled Optical Properties. Proc. Natl. Acad. Sci. U. S. A. 2016, 113, 5275−5280.

(21) Aldana, J.; Wang, Y. A.; Peng, X. Photochemical Instability of CdSe Nanocrystals Coated by Hydrophilic Thiols. J. Am. Chem. Soc. 2001, 123, 8844−8850.

(22) Grabolle, M.; Spieles, M.; Lesnyak, V.; Gaponik, N.; Eychmüller, A.; Resch-Genger, U. Determination of the Fluorescence Quantum Yield of Quantum Dots: Suitable Procedures and Achievable Uncertainties. Anal. Chem. 2009, 81, 6285−6294.

(23) Baskoutas, S.; Terzis, A. F. Size-Dependent Band Gap of Colloidal Quantum Dots. J. Appl. Phys. 2006, 99, 013708.

(24) Yu, W. W.; Qu, L.; Guo, W.; Peng, X. Experimental Determination of the Extinction Coefficient of CdTe, CdSe, and CdS Nanocrystals. Chem. Mater. 2003, 15, 2854−2860.

(25) Peng, X.; Schlamp, M. C.; Kadavanich, A. V.; Alivisatos, A. P. Epitaxial Growth of Highly Luminescent CdSe/CdS Core/Shell Nanocrystals with Photostability and Electronic Accessibility. J. Am. Chem. Soc. 1997, 119, 7019−7029.

(26) Xie, R.; Kolb, U.; Li, J.; Basché, T.; Mews, A. Synthesis and Characterization of Highly Luminescent CdSe−Core CdS/$Zn_{0.5}Cd_{0.5}$S/ZnS Multishell Nanocrystals. J. Am. Chem. Soc. 2005, 127, 7480−7488.

(27) Lee, H. J.; Yum, J.; Leventis, H. C.; Zakeeruddin, S. M.; Haque, S. A.; Chen, P.; Seok, S. I.; Gratzel, M.; Nazeeruddin, M. K. CdSe Quantum Dot-Sensitized Solar Cells Exceeding Efficiency 1% at Full-Sun Intensity. J. Phys. Chem. C 2008, 112, 11600−11608.

(28) Shen, Q.; Kobayashi, J.; Diguna, L. J.; Toyoda, T. Effect of ZnS Coating on the Photovoltaic Properties of CdSe Quantum Dot-Sensitized Solar Cells. J. Appl. Phys. 2008, 103, 084304.

(29) Huber, R. E.; Criddle, R. S. Comparison of the Chemical Properties of Selenocysteine and Selenocystine with their Sulfur Analogs. Arch. Biochem. Biophys. 1967, 122, 164−173.

(30) Esaki, N.; Nakamura, T.; Tanaka, H.; Suzuki, T.; Morino, Y.; Soda, K. Enzymic Synthesis of Selenocysteine in Rat Liver. Biochemistry 1981, 20, 4492−4496.
(31) Pu, C.; Peng, X. To Battle Surface Traps on CdSe/CdS Core/ Shell Nanocrystals: Shell Isolation Versus Surface Treatment. J. Am. Chem. Soc. 2016, 138, 8134−8142.
(32) Chen, O.; Zhao, J.; Chauhan, V. P.; Cui, J.; Wong, C.; Harris, D. K.; Wei, H.; Han, H.; Fukumura, D.; Jain, R. K.; Bawendi, M. G. Compact high-quality CdSe-CdS core-shell nanocrystals with narrow emission linewidths and suppressed blinking. Nat. Mater. 2013, 12, 445−451.
(33) Leatherdale, C. A.; Woo, W.; Mikulec, F. V.; Bawendi, M. G. On the Absorption Cross Section of CdSe Nanocrystal Quantum Dots. J. Phys. Chem. B 2002, 106, 7619−7622.
(34) Rice, K. P.; Saunders, A. E.; Stoykovich, M. P. Seed-Mediated Growth of Shape-Controlled Wurtzite CdSe Nanocrystals: Platelets, Cubes, and Rods. J. Am. Chem. Soc. 2013, 135, 6669−6676.
(35) Li, J. J.; Wang, Y. A.; Guo, W.; Keay, J. C.; Mishima, T. D.; Johnson, M. B.; Peng, X. Large-Scale Synthesis of Nearly Monodisperse CdSe/CdS Core/Shell Nanocrystals Using Air-Stable Reagents via Successive Ion Layer Adsorption and Reaction. J. Am. Chem. Soc. 2003, 125, 12567−12575.
(36) Qian, H.; Li, L.; Ren, J. One-step and Rapid Synthesis of High Quality Alloyed Quantum Dots (CdSe−CdS) in Aqueous Phase by Microwave Irradiation with Controllable Temperature. Mater. Res. Bull. 2005, 40, 1726−1736.
(37) Kalasad, M.; Rabinal, M.; Mulimani, B. Ambient Synthesis and Characterization of High-Quality CdSe Quantum Dots by an Aqueous Route. Langmuir 2009, 25, 12729−12735.